



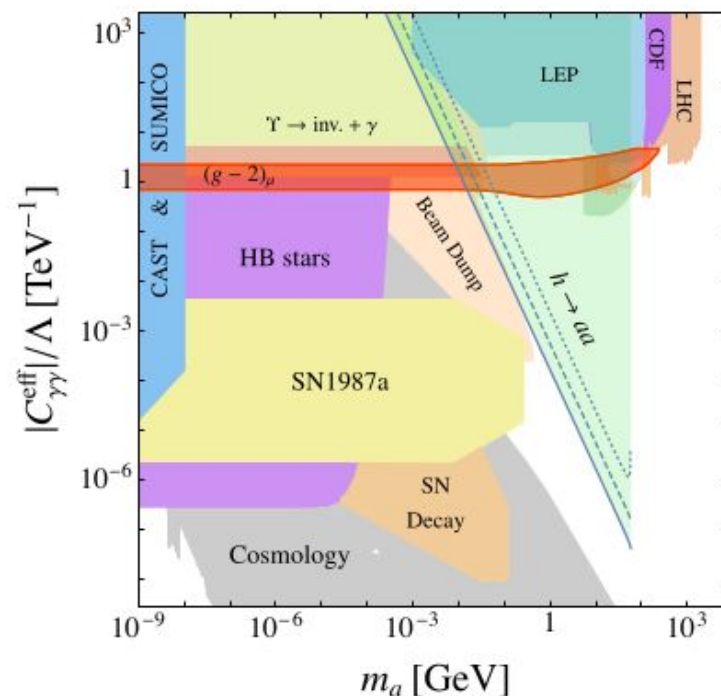
**Search for ALPs in Higgs boson  
decays in ATLAS**

Olivera Vujanović  
on behalf of the ATLAS Collaboration

- Introducing light scalar or pseudo-scalar axion like particles (ALPs) could explain:
  - Strong CP problem
  - Dark matter
  - $(g-2)_\mu$  discrepancy

$$\begin{aligned}
 a_\mu^{(\text{exp})} &= (g_\mu - 2)^{(\text{exp})}/2 \\
 &= 116592091(63) \times 10^{-11} \quad [1] \\
 a_\mu^{(\text{theo})} &= 116591823(49) \times 10^{-11} \quad [2-4]
 \end{aligned}$$

- Probing unconstrained  $m_a - C_W$  parameter space:
  - $(gg)H \rightarrow aa \rightarrow \gamma\gamma\gamma$
  - $100 \text{ MeV} \leq m_a \leq 62 \text{ GeV}$
  - $1e-5 \leq C_W \leq 1$
- Deriving upper limits on ALP cross-section & excluding  $m_a - C_W$  combinations



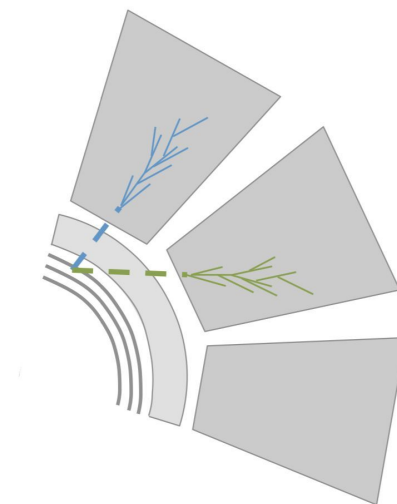
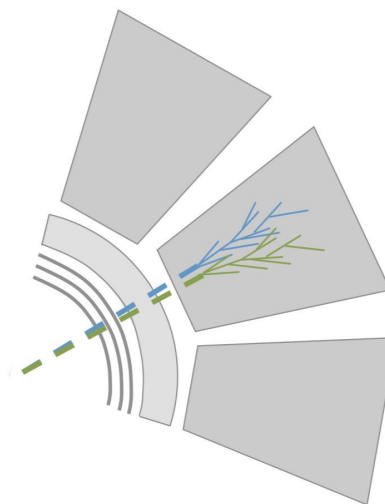
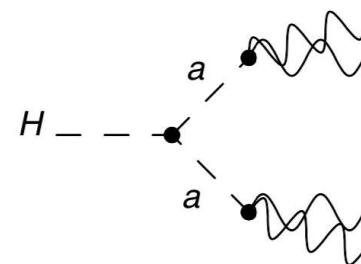
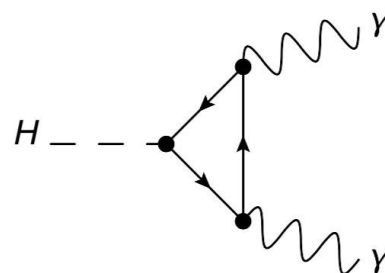
M. Bauer, M. Neubert, and A. Thamm, J. High Energ. Phys. 2017, 44 (2017)

[1] G. W. Bennett, Phys. Rev. D 73, 072003 (2006)  
 [2] A. Kurz, T. Liu, P. Marquard, A. V. Smirnov, V. A. Smirnov, and M. Steinhauser, Phys. Rev. D 93, 053017 (2016)  
 [3] T. Kinoshita and M. Nio, Phys. Rev. D 73, 053007 (2006)  
 [4] T. Aoyama, M. Hayakawa, T. Kinoshita, and M. Nio, Phys. Rev. Lett. 99, 110406 (2007)

- Experimentally challenging signatures

$$\Gamma_{a\gamma\gamma} = \frac{4\pi\alpha^2 m_a^3}{\Lambda^2} |C_{a\gamma\gamma}|^2$$

- ALPs with long lifetimes can decay close to the calorimeter
  - Detector design and photon reconstruction is optimized for photons from primary vertex
  - Reduced reconstruction efficiency
- Requiring that axions decay within ECal (< 1970 mm)
- Low mass ALPs: highly collimated photon pairs  $\Rightarrow$  reconstructed as one photon (“merged”)



- **Photon ID** based on 2 NNs (each with 2 hidden layers - 7 and 5 nodes; with shower shapes used as input variables):

**NN1: real vs. fake photons**

- Signal:  $H \rightarrow aa$ ,  $H \rightarrow \gamma\gamma$
- Background: selected data with photons such that  $p_T > 15$  GeV, fail loose ID, isolated ( $ETCone40/p_T < 0.1$ ),  $m_{inv} > 60$  GeV (Higgs region excluded)

**NN2: merged vs. single photons**

- Signal:  $H \rightarrow aa \rightarrow \gamma\gamma\gamma\gamma$  merged photons
- Background:  $H \rightarrow aa \rightarrow \gamma\gamma\gamma\gamma$  single photons

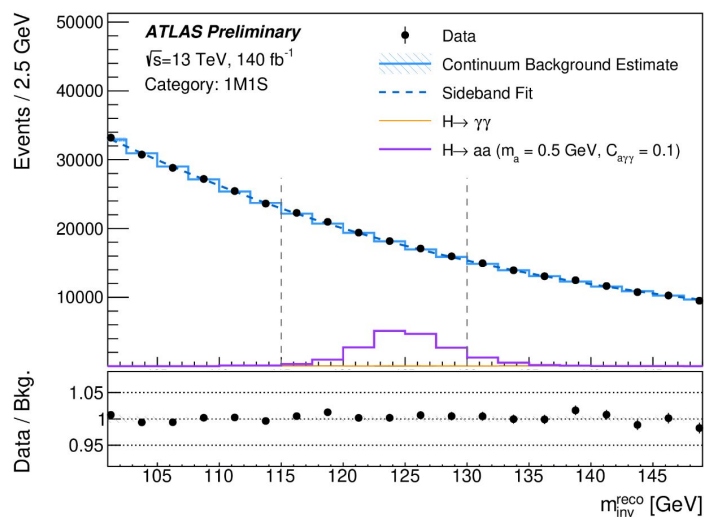
- Each photon gets one of 3 labels:
  - merged ( $ANN1 > 0.98$ ,  $ANN2 > 0.5$ ,  $I_{tight}$ )
  - loose
  - tight

- Resulting in 5 categories:
  - **4S**: 4 loose photons, at least 1 ( $\geq 3$ ) tight photon
  - **3S**: 2 tight + 1 loose photons
  - **2M**: 2 merged photons
  - **1M1S**: 1 merged + 1 loose photon
  - **2S**: 2 tight photons (dominated by  $H \rightarrow \gamma\gamma$  background)
- **Axion mass reconstruction**: only possible in 3S and 4S categories; used to define SR and CR (by inverting the axion mass requirement)
- 2 NNs for each case:
  - Input:  $m_{\text{inv}}$  of all possible di-photon combinations, pairwise differences in  $p_T$ , pairwise differences in direction
  - Labels based on MC truth information

**Prompt analysis ( $4S_p$ )**: more stringent categorization criteria (loosened needed for long-lived case as ID efficiency drops for axions decaying closer to the ECal)

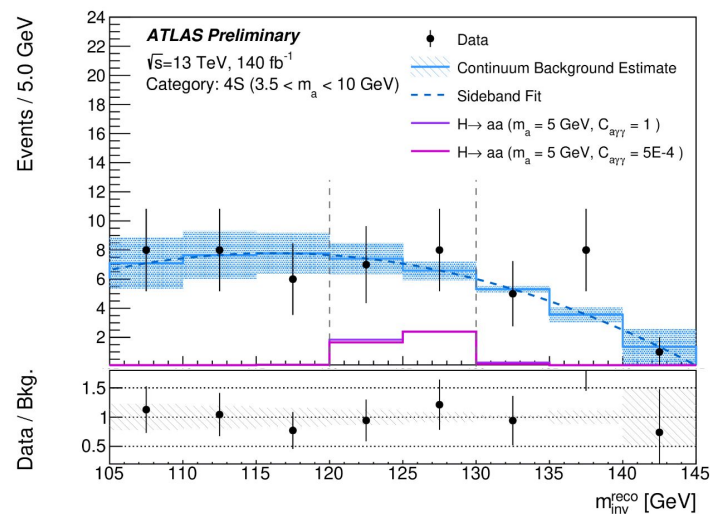
## 2-photon final states

- Using a sideband in  $m_H$  distribution to fit the background contribution in [100, 150] GeV, excluding signal region
- Used fit functions:
  - 2S and 1M1S: Landau
  - 2M: Polynomial of 2<sup>nd</sup> order
- Cross-checks:
  - 2y QCD MC
  - data driven: inverted isolation cut



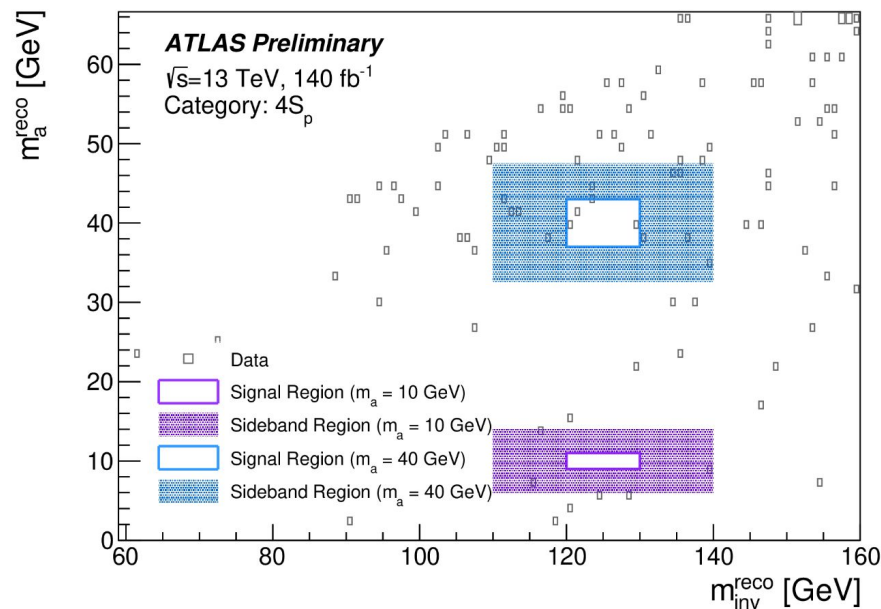
## 3- and 4-photon final states

- Using a sideband in  $m_H$  distribution to fit the background contribution in [80, 150] GeV and [105, 145] GeV for 3S and 4S respectively, excluding signal region
- Used fit functions:
  - Polynomial of 3<sup>rd</sup> and 2<sup>nd</sup> order
- Cross-checks:
  - 3y, 4y QCD MC
  - data driven: inverted axion mass requirement



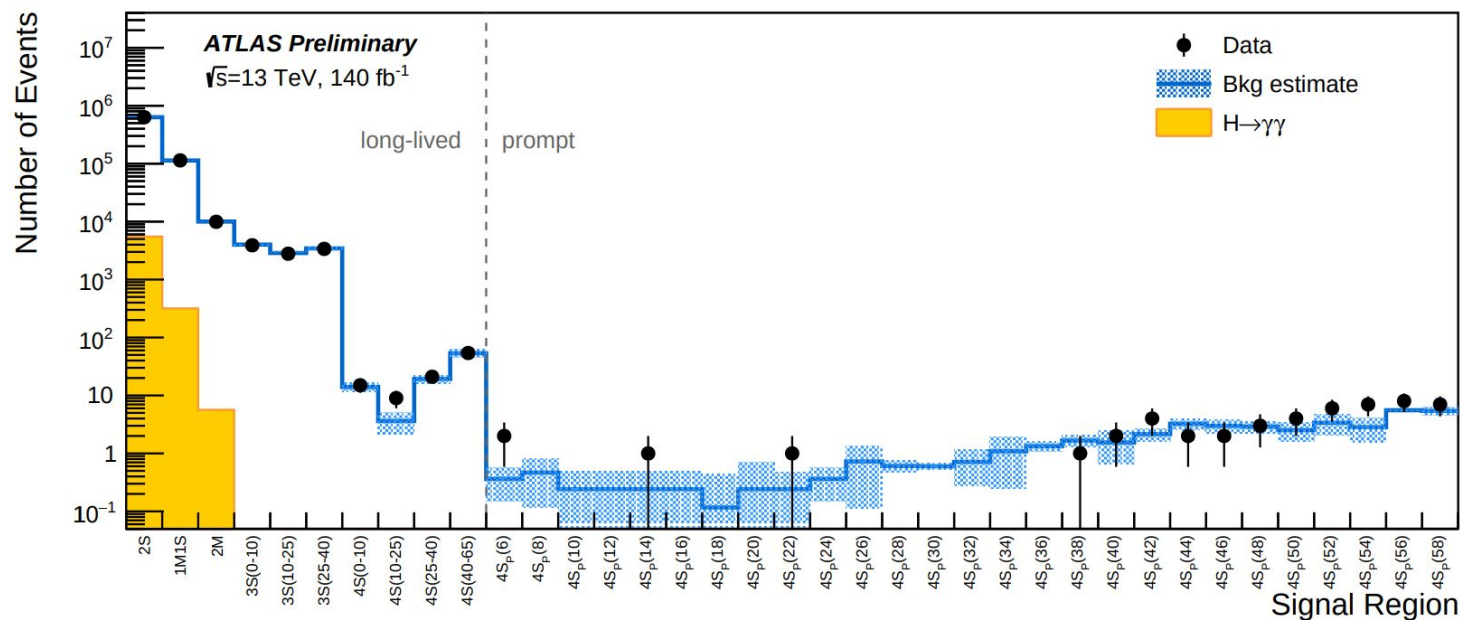
## Prompt final states

- Considering only  $4S_p$  case with  $m_a > 5\text{ GeV}$ ; low statistics due to harsher rejection of fake photon signatures
- Using a 2D sideband fit approach with the  $m_H^{\text{reco}}$  vs.  $m_a^{\text{reco}}$  spectra with SR and CR defined as:
  - SR:  $120\text{ GeV} < m_H < 130\text{ GeV}$  and  $m_a$  in  $m_a \pm \text{stepsize}$
  - CR1:  $110\text{ GeV} < m_H < 140\text{ GeV}$  and  $m_a$  in  $m_a \pm \text{stepsize} * 1.5$
  - CR2:  $105\text{ GeV} < m_H < 145\text{ GeV}$  and  $m_a$  in  $m_a \pm \text{stepsize} * 2.5$
- Background estimated as an average of data events in the CR



[ATLAS-CONF-2023-040]

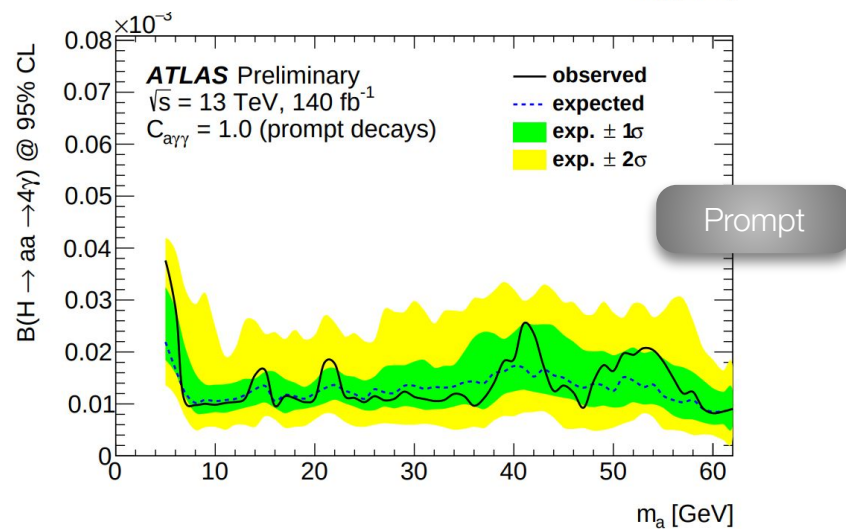
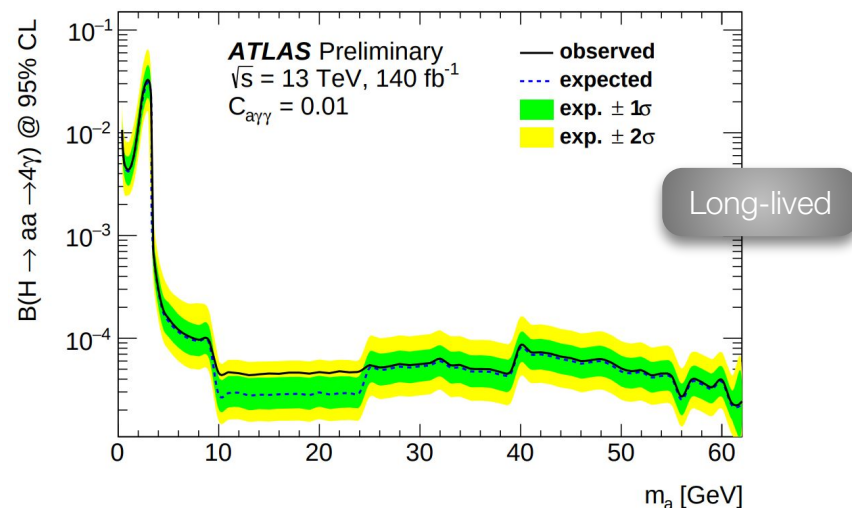
- Overview of estimated background events compared to measured data events in the signal region of the most sensitive categories
- The  $H \rightarrow \gamma\gamma$  background is only visible in the first three bins, corresponding to the 2-photon categories



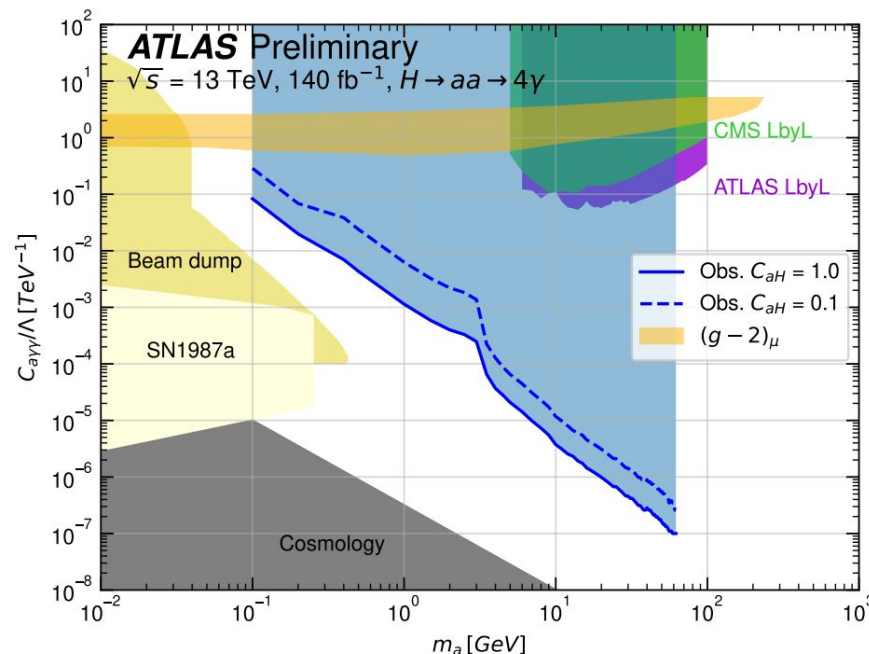


## Limits

- Setting upper limits on  $B(H \rightarrow aa \rightarrow 4\gamma)$  at 95% CL as a function of the axion mass and for different ALP-photon couplings
- The long-lived searches significantly less sensitive than the prompt searches due to the looser signal selection and consequently larger background contributions
- The observed limits agree well with the expected limits.

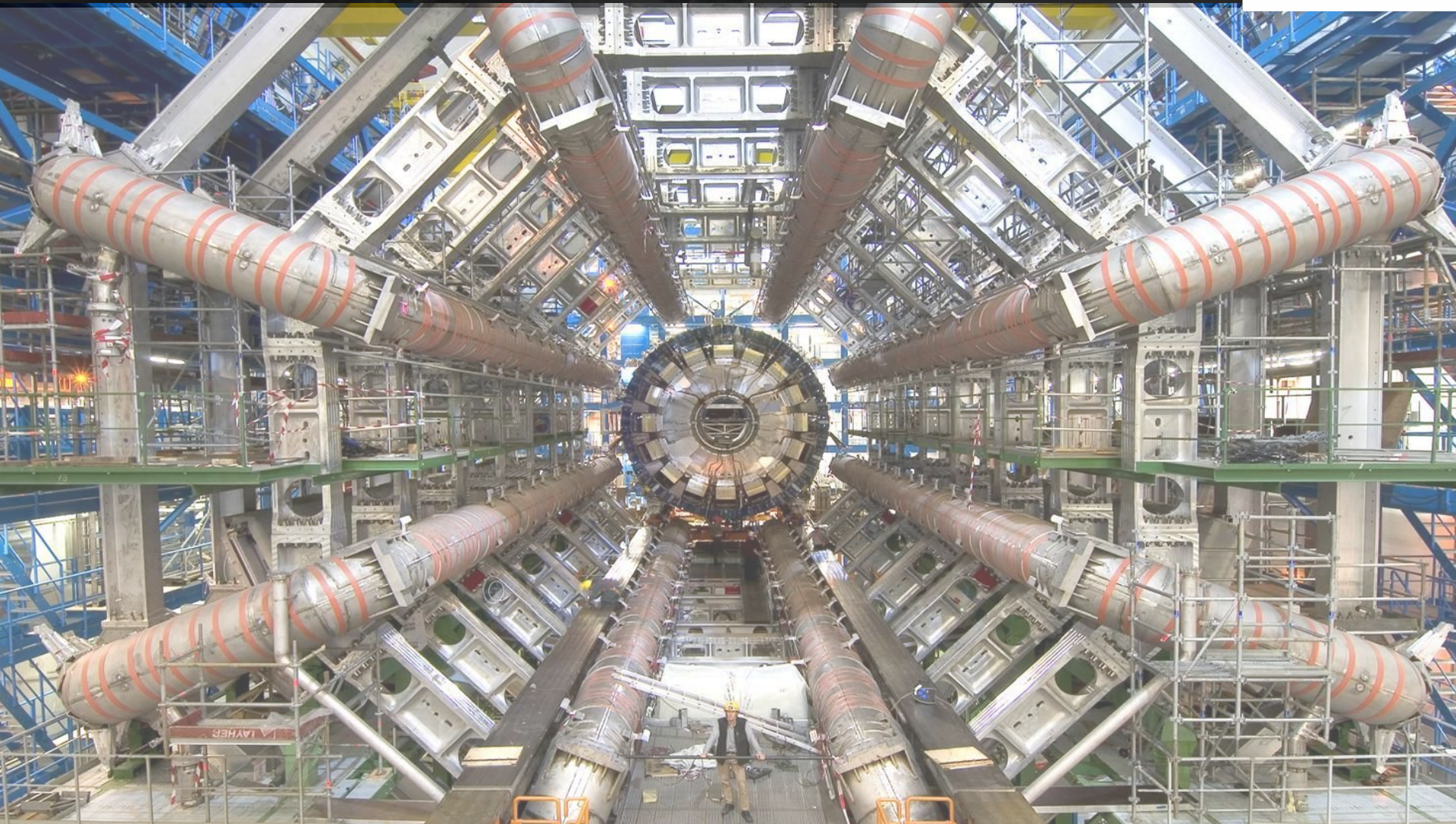


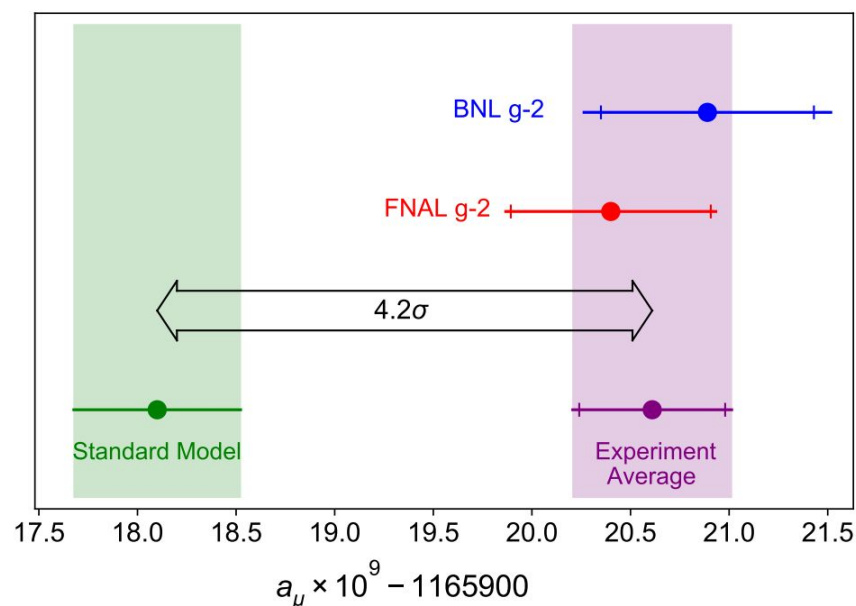
- Limits on ALP masses with  $m_a > 15$  GeV:
  - ~ one order of magnitude more stringent than previous ATLAS analyses using 8 TeV data
  - similar to slightly better sensitivity as previous analyses from CMS using  $132 \text{ fb}^{-1}$  of  $\sqrt{s} = 13$  TeV data
- First limits on ALPs with masses  $< 10$  GeV derived at ATLAS
  - 40% more stringent compared to the previous results from CMS using  $136 \text{ fb}^{-1}$  of  $\sqrt{s} = 13$  TeV
- **Most stringent limits to date**
- Excluded most of the remaining parameter space that could explain the  **$(g-2)_\mu$  discrepancy**



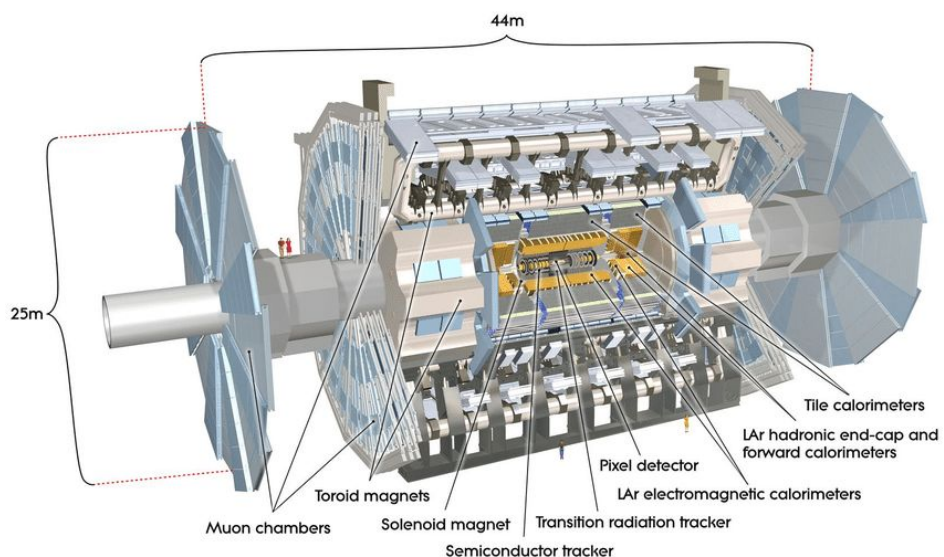
Limits on the ALP mass and coupling to photons at 95% CL, assuming  $|C_{aH}^{eff}/\Lambda^2| = 1 \text{ TeV}^{-2}$  (solid line) and  $|C_{aH}^{eff}/\Lambda^2| = 0.1 \text{ TeV}^{-2}$  (dashed line)

[ATLAS-CONF-2023-040]

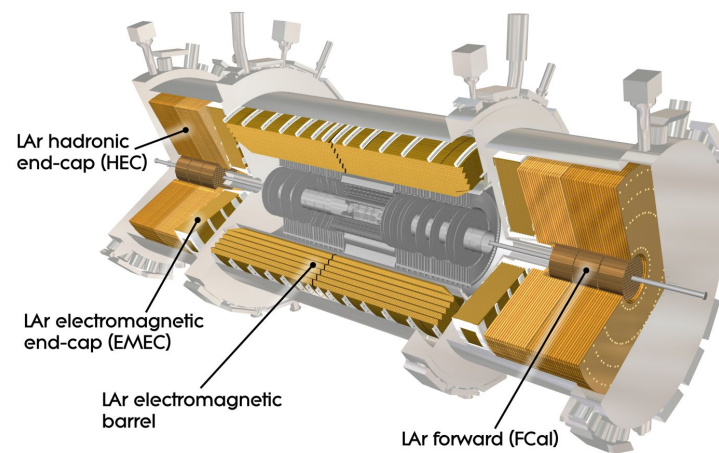




- *Measurement of the Positive Muon Anomalous Magnetic Moment to 0.46 ppm*  
(<https://arxiv.org/pdf/2104.03281.pdf>)
- First results of the Fermilab Muon  $g-2$  Experiment for the positive muon magnetic anomaly  $a_\mu \equiv (g_\mu - 2)/2$ .
- From top to bottom: experimental values of  $a_\mu$  from BNL E821, this measurement, and the combined average. The inner tick marks indicate the statistical contribution to the total uncertainties. The Muon  $g-2$  Theory Initiative recommended value for the standard model is also shown.



Calorimeter system



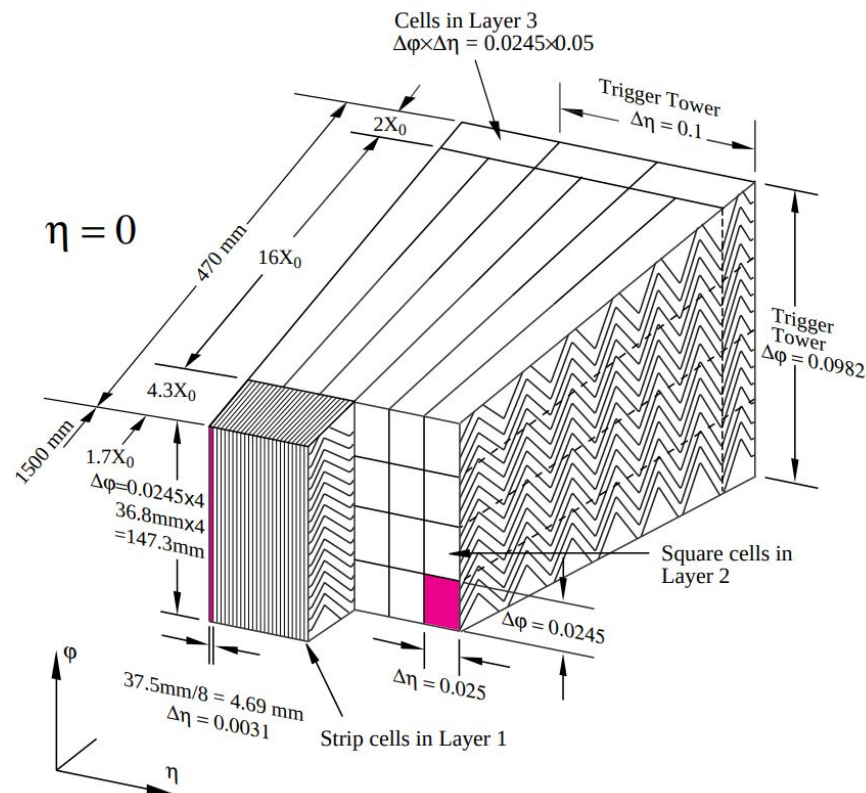
## ■ Liquid argon calorimeter (LAr)

- specially designed to identify electrons and photons; honeycomb pattern
- kept at  $-184^{\circ}\text{C}$
- features layers of metal (either tungsten, copper or lead) that absorb incoming particles, converting them into a “shower” of new, lower energy particles, which ionise liquid argon sandwiched between the layers, producing an electric current that is measured

[ATLAS-CONF-2023-040]

- 9 discriminating variables (DVs) based on energy in cells of ECAL and leakage in hadronic calorimeter HCAL
  
- Loose ID:
  - exploits the DVs in the HCAL and in the ECAL middle layer
  - used by triggers or as background control region
  
- Tight ID:
  - tighter cuts on DVs than the ones used by Loose ID
  - using also ECAL strip layer
  - used for offline analysis

- Sketch of a barrel module with the granularity of cells depicted in  $\eta$  and  $\phi$



- 9 discriminating variables (DVs) based on energy in cells of ECAL and leakage in hadronic calorimeter HCAL

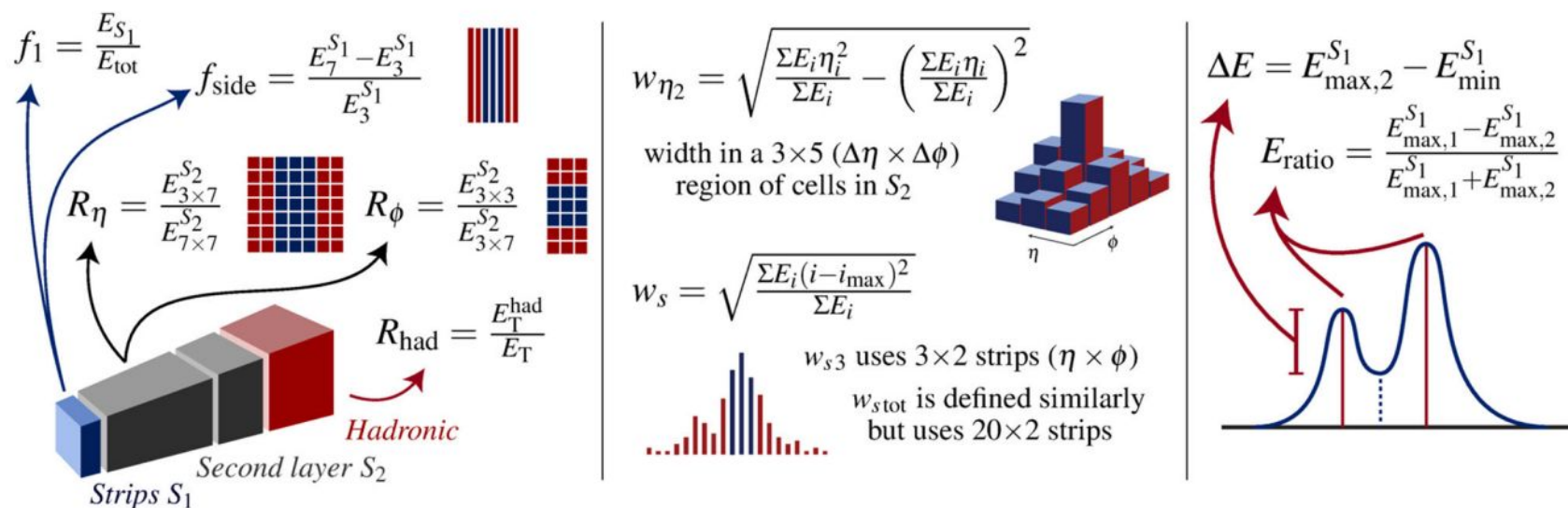
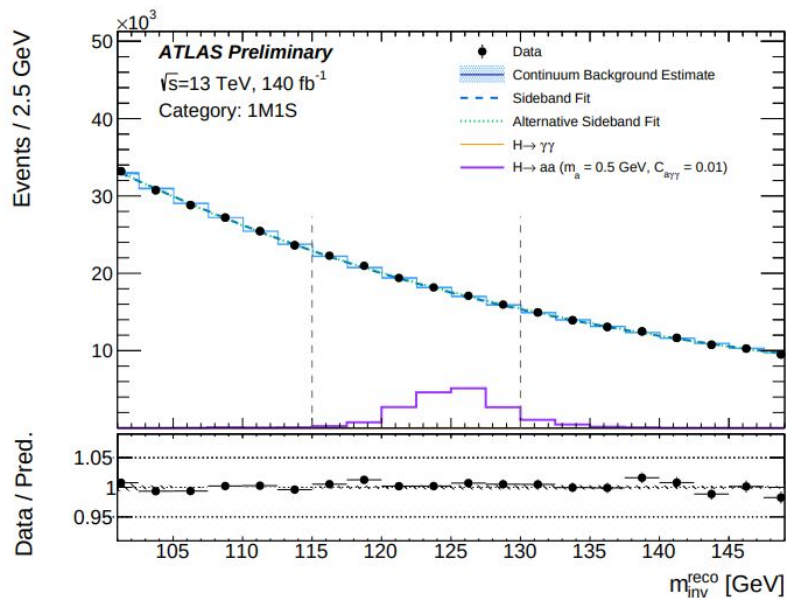
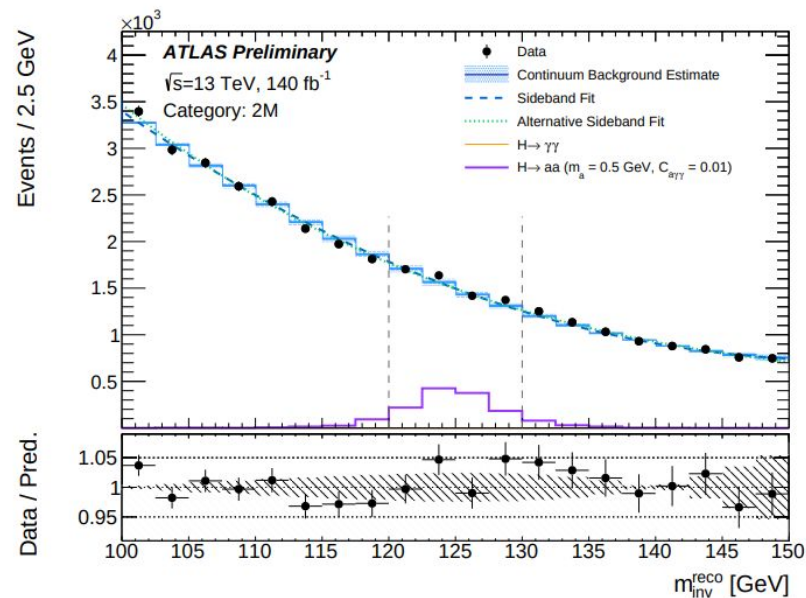


**Fig. 2** Schematic representation of the photon identification discriminating variables, from Ref. [23].  $E_C^{S_N}$  identify the electromagnetic energy collected in the  $N$ -th longitudinal layer of the electromagnetic

calorimeter in a cluster of properties  $C$ , identifying the number and/or properties of selected cells.  $E_i$  is the energy in the  $i$ -th cell,  $\eta_i$  the pseudorapidity centre of that cell



(a)

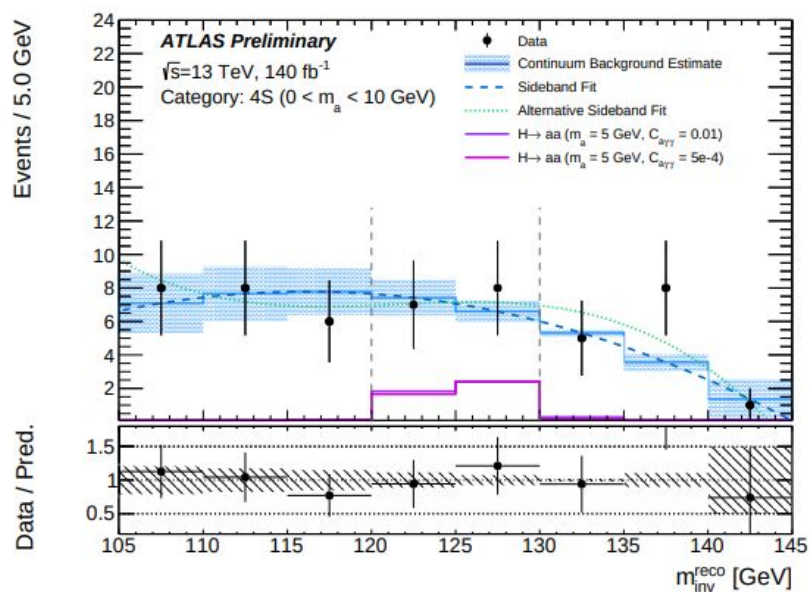


(b)

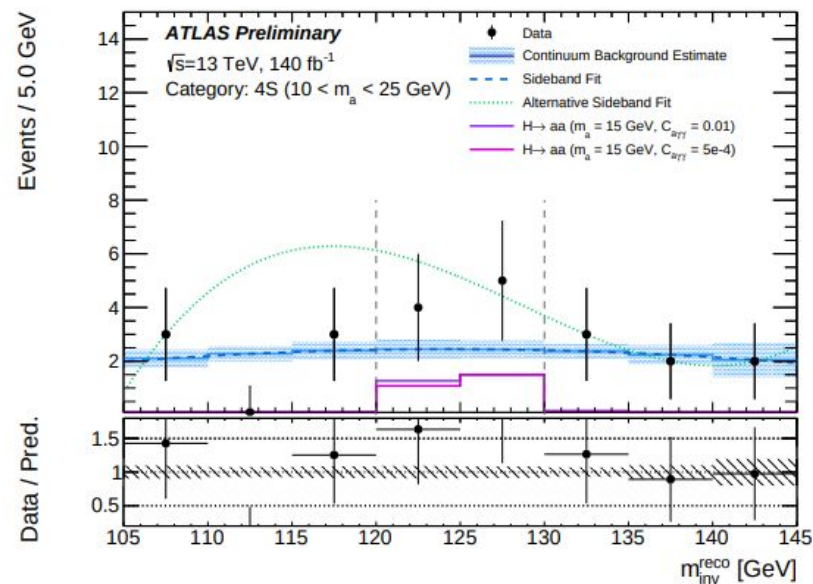
Figure 1:  $m_{\text{inv}}^{\text{reco}}$  distribution for the nominal signal selection for the (a) 1M1S, and (b) 2M category. The nominal sideband fitting function as well as its systematic variation is shown for both cases. The expected signal shape for  $C_{\text{a}\gamma\gamma} = 0.1$  is also shown with an arbitrary normalization. The signal region selection on  $m_{\text{inv}}^{\text{reco}}$  is indicated as dashed lines.



[ATLAS-CONF-2023-040]

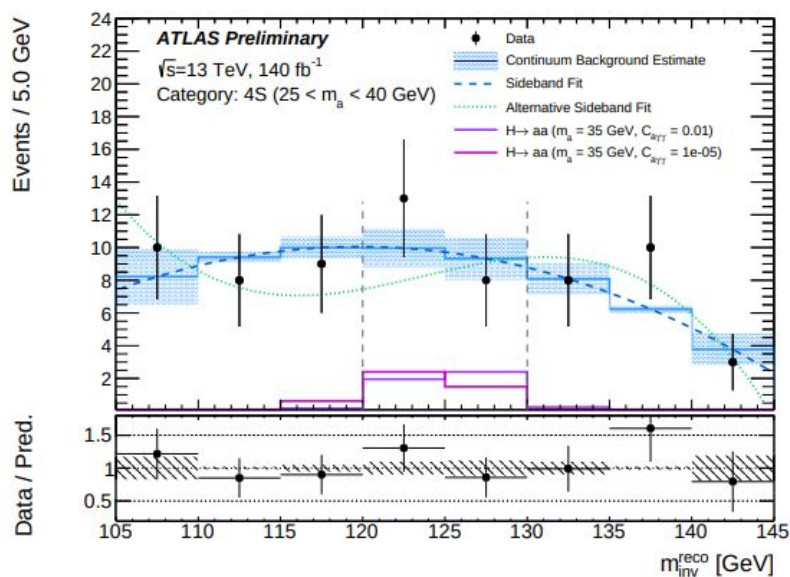


(a)

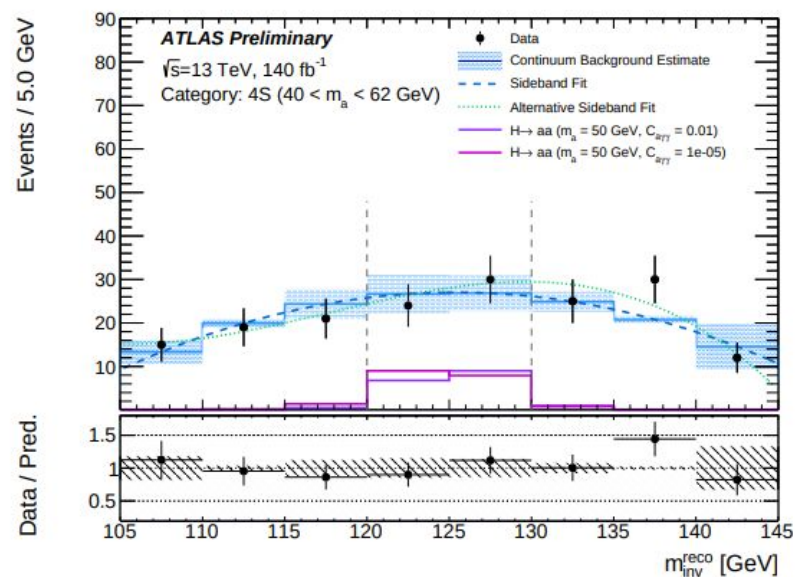


(b)

[ATLAS-CONF-2023-040]



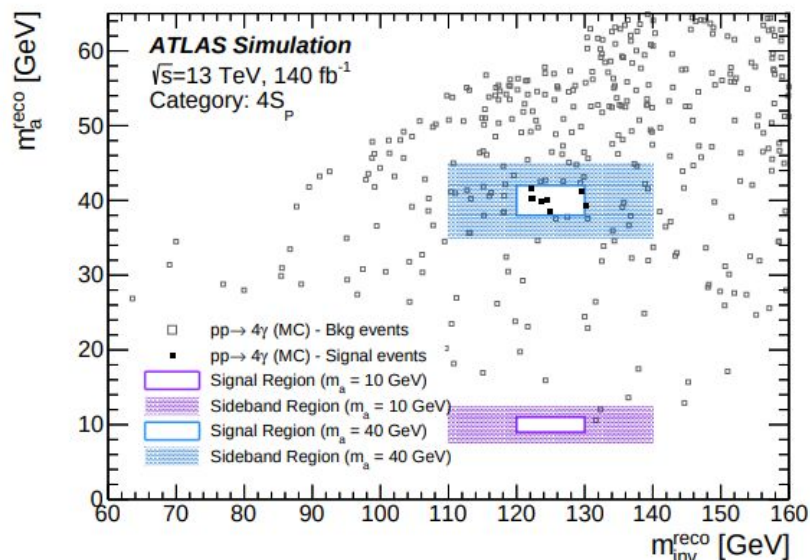
(c)



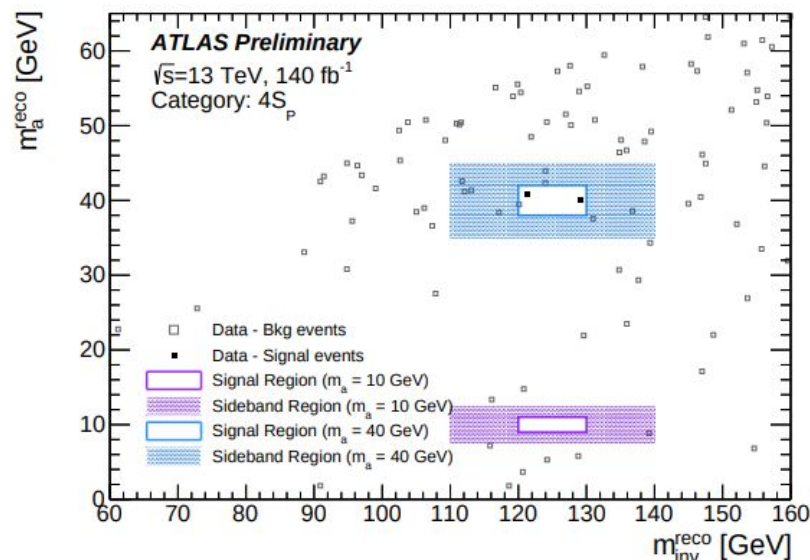
(d)

Figure 2: 4S category in the search for long-lived ALPs:  $m_{\text{inv}}^{\text{reco}}$  distribution for the nominal signal selection including the nominal and alternative sideband fitting functions, the estimated background from the sideband fit in the signal region as well as the expected signal shape for two ALP-photon couplings with arbitrary normalization. The 4 plots show different ALP mass ranges: (a)  $0 < m_a < 10$  GeV, (b)  $10 < m_a < 25$  GeV, (c)  $25 < m_a < 40$  GeV, (d)  $40 < m_a < 62$  GeV. The signal region selection on  $m_a^{\text{reco}}$  is applied while the signal region selection on  $m_{\text{inv}}^{\text{reco}}$  is indicated as dashed lines.

[ATLAS-CONF-2023-040]



(a) MC



(b) Data

Figure 3:  $m_{\text{inv}}^{\text{reco}}$  vs.  $m_a^{\text{reco}}$  for the  $4S_p$  categories in the search for promptly decaying ALPs, for (a) simulated  $pp \rightarrow 4\gamma$  sample and (b) for data. The signal (sideband) regions are indicated as solid lines (shaded areas) for the searches for ALPs with masses of 10 and 40 GeV.

[ATLAS-CONF-2023-040]

## Nominal uncertainties

- Nominal (as recommended) systematic uncertainties are evaluated for:
  - Lumi 0.8%
  - Pileup  $< 1\%$
  - Trigger 2% - 3%
  - Photon ID, ISO, scale, resolution  $\leq 3\%$  on selected events

## Custom uncertainties

- Special attention paid to the systematic uncertainties due to displaced vertices and their effect on the shower shapes
- Using cluster shapes associated to tracks from displaced vertices of long lived hadrons (kaons) - data and MC
- 3 regions:
  - **near:**  $z_0 < 20$  mm,  $d_0 < 1$  mm
  - **medium:**  $20$  mm  $< z_0 < 500$  mm,  $1$  mm  $< d_0 < 80$  mm
  - **far:**  $500$  mm  $< z_0$ ,  $d_0 > 80$  mm
- NN classifiers:
  - $Z \rightarrow ee$  events used comparing MC and data, electron shower shape variables used as inputs
  - Difference propagated through analysis: up to 15% normalisation uncertainty in the 2M and 1M1S categories